

PCCP

Accepted Manuscript



This is an *Accepted Manuscript*, which has been through the Royal Society of Chemistry peer review process and has been accepted for publication.

Accepted Manuscripts are published online shortly after acceptance, before technical editing, formatting and proof reading. Using this free service, authors can make their results available to the community, in citable form, before we publish the edited article. We will replace this *Accepted Manuscript* with the edited and formatted *Advance Article* as soon as it is available.

You can find more information about *Accepted Manuscripts* in the [Information for Authors](#).

Please note that technical editing may introduce minor changes to the text and/or graphics, which may alter content. The journal's standard [Terms & Conditions](#) and the [Ethical guidelines](#) still apply. In no event shall the Royal Society of Chemistry be held responsible for any errors or omissions in this *Accepted Manuscript* or any consequences arising from the use of any information it contains.

Absolute Configuration and Chiral Self-Assembly of Rubrene on Bi(111)

Kai Sun, Meng Lang, Jun-Zhong Wang*

School of Physical Science and Technology & MOE Key Lab Luminescence & Real Time Anal, Southwest University, Chongqing 400715, China.

We investigated the chiral self-assembly of rubrene molecules on a semi-metallic Bi(111) surface using low-temperature scanning tunneling microscopy. The absolute configuration of isolated rubrene enantiomers was identified from high-resolution images. Two types of homochiral domains of rubrene monomers and hexamers were observed, respectively. For rubrene monomers, chiral separation was spontaneous with each chiral monomer appearing in their respective domain. For rubrene hexamers, two levels of organization chirality were recorded: one is six heterochiral rubrene molecules arranged alternatively in a rubrene hexamer; and the other is a homochiral arrangement of individual hexamers. After annealing at 350 K, a large area of supramolecular self-assembled L- and R-type triangular heterochiral hexamers were obtained at the narrow terrace of Bi(111). Moreover, a molecular chiral inversion from L-(R-)type to R-(L-)type occurs during the formation of the hexamer domain structure and can be attributed to the enhanced intermolecular interactions governed by the intensive intermolecular extrusion at the narrow terrace.

Introduction

As a universal phenomenon in nature, chirality plays an important role in physics, chemistry, life science as well as material science. In particular, chirality at 2D surfaces has attracted considerable attention over the past few years due to its potential applications in enantioselective catalysis, enantiospecific sensors and non-linear optical devices [1-4]. A series of significant achievements have been made on 2D chirality such as chiral recognition [5-7], chiral separation [8-12] and chiral construction [13-15]. Chiral and achiral molecules can assemble into supramolecular chiral structures on the surface when the surface symmetry is broken [16].

Rubrene (5,6,11,12-tetraphenyltetracene, $C_{42}H_{28}$), an axial chiral molecule that consists of a twisted tetracene backbone with four phenyl substituents symmetrically attached to the two sides of the backbone in the gas phase (Fig. 1a and b), has been

widely employed in light-emitting diodes and field-effect transistors because of the higher charge carrier mobility of rubrene single crystals on the surface [17-21]. The twisted tetracene backbone can lead to chiral adsorption when the rubrene molecule is deposited on a solid surface. However, rubrene crystals adopt a planar tetracene backbone without any chirality [22]. So far, various chiral structures of rubrene have been investigated on different solid surfaces. Schneider et al. reported the existence of local chiral and hierarchical chiral structures of rubrene [23-26]. Li Wang et al. observed supramolecular chiral self-assembly of rubrene on Au(111) [27]. Rosei et al. investigated the self-assembly of rubrene on copper surfaces [22, 28-29] and found the coexistence of achiral row-like and chiral square-like assemblies [29]. However, these studies mentioned above were performed on noble metal surfaces. It was reported recently that pentacene, another benchmark molecule, grown on the semimetallic Bi(111) substrate forms the epitaxial crystalline films with pentacene molecule standing up, even in the first monolayer[30,31]. The upright orientation of the pentacene molecule is attributed to the small density of states near the Fermi level, which leads to the reduction of molecule-substrate interaction[32]. In the present study, we present the chiral adsorption of isolated rubrene molecules adsorbed on a Bi(111) surface and low-temperature scanning tunneling microscopy (STM) was used to evaluate its chiral separation and self-assembly. The triangular hexamers may show clockwise (R) or anticlockwise (L) handedness at the narrow terrace. Moreover, the strong intermolecular forces originating from the repulsive interactions between rubrene molecules may cause a molecular chiral reversal, which is also investigated.

Experimental

The experiments were carried out in a Unisoku low-temperature scanning tunneling microscopy (STM) system with base pressure of 1.0×10^{-10} mbar. Flat and well-ordered Bi(111) films were prepared by depositing 20 monolayers of bismuth atoms on a Si(111) 7×7 surface at room temperature with subsequent annealing at 400 K. Rubrene molecules were deposited onto Bi(111) surface by heating the tantalum cell to 473 K in an ultra-high vacuum while the sample was held at 100 K. The typical growth rate was about 0.03 monolayers per minute. The sample was transferred into the STM chamber immediately after the deposition of rubrene molecules. Constant current STM images were acquired at a liquid helium

temperature of 4.3 K. Throughout this study, we define the rubrene coverage in terms of the crystalline monolayer corresponding to the a–b plane of rubrene single crystals.

Results and discussion

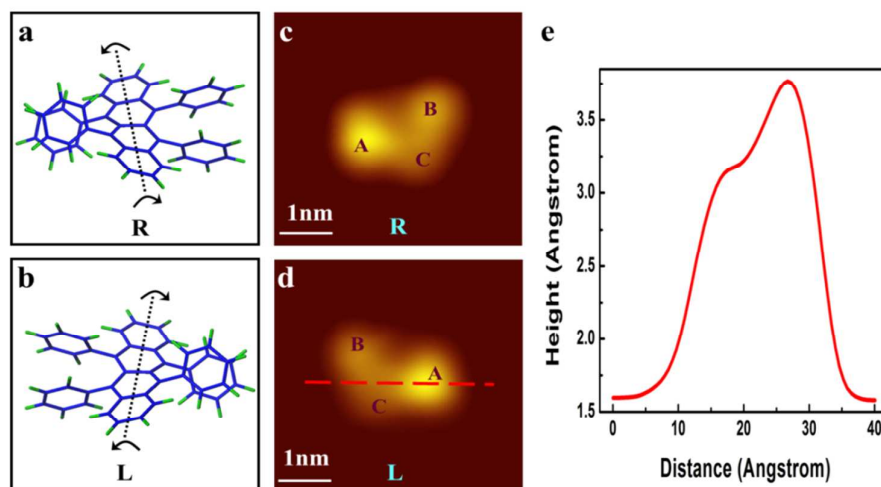


Fig. 1 Isolated rubrene molecules of opposing handedness. Chemical structure of (a) R- and (b) L-type monomer of rubrene. High-resolution STM image of (c) R- and (d) L-type monomers of rubrene, 4.7 nm \times 4.7 nm, +2.0 V. (e) The height profile line across the Rubrene molecule marked with a dashed line in (d).

Firstly, a small amount of rubrene molecules were deposited onto a Bi(111) surface at a low temperature, and individual rubrene molecules were observed on the terrace as shown in Figs. 1c and d. Each isolated molecule exhibits an apparent height of approximately 0.23 nm (Figs. 1e) and consists of three unequally shaped features (denoted by A, B and C) with heights decreasing from A to C. The height of features B and C is approximately 22 and 38% lower than A. These height ratios were acquired from plenty of rubrene monomers and determine the molecular chirality. The left molecule in Fig. 1c presents a clockwise arrangement of ABC, whereas the right one in Fig. 1d follows an anticlockwise orientation of BAC. The rubrene molecules have a mirrored symmetry with respect to each other. They were classified as R- and L-enantiomers, which demonstrates the chiral conformations of rubrene molecules in

the gas phase. In addition, the chiral adsorption of single rubrene molecules on the Bi(111) surface is very similar to that on Au(111) [24], which implies the molecules may adopt identical adsorption orientations on both surfaces.

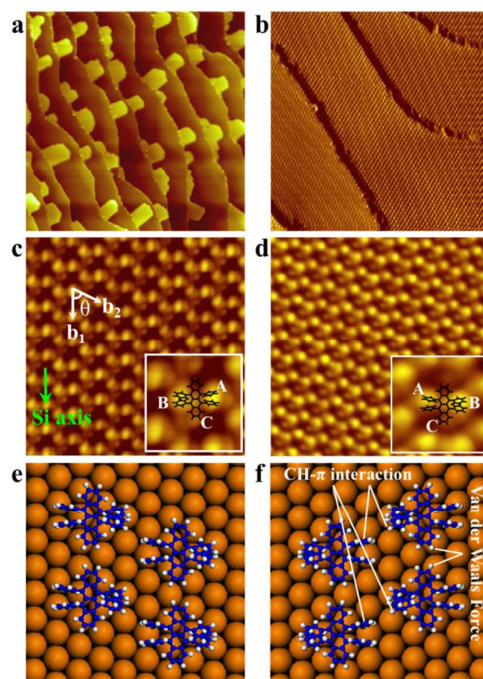


Fig. 2 Homochiral domains of rubrene monomers formed on Bi(111). (a) Sub-monolayer rubrene islands sticking to the step edges of the substrate, $300 \text{ nm} \times 300 \text{ nm}$, $+5.4 \text{ V}$. (b) Full monolayer rubrene on Bi(111) with a moiré pattern, $128 \text{ nm} \times 128 \text{ nm}$, $+2.0 \text{ V}$. High-resolution STM images acquired on the (c) L- and (d) R-type domains and structure models, $15 \text{ nm} \times 15 \text{ nm}$, $+2.0 \text{ V}$. (e) Schematic diagrams of structural models for the (e) L- and (f) R-type homochiral domains.

With increasing coverage, rubrene molecules begin to assemble into sub-monolayer islands at the step edges (Fig. 2a) of the Bi(111) substrate because of the strong attractive force from the step edge. When the coverage reaches one monolayer, the homochiral domain showed a widely recognized moiré pattern characterized by a 4×3 supercell (Fig. 2b). The lattice of the homochiral domain was $b_1 = 14.6 \pm 0.2 \text{ \AA}$, $b_2 = 16.6 \pm 0.2 \text{ \AA}$, $\theta = 68.0 \pm 0.5^\circ$. b_1 is parallel to a principal axis of the Bi(111) substrate,

and the packing density is calculated to be $\approx 0.445 \text{ nm}^{-2}$. The homochiral domain can be classified into two structures with opposing chirality from the high-resolution images. One is an L-type domain composed of only L-rubrene molecules, and the other is an R-type domain consisting of uniform R-rubrene molecules, which revealed a spontaneous chiral separation occurring on Bi(111) surface. Within the homochiral domain, each rubrene molecule retained chirality with a twisted tetracene backbone resembling the chiral adsorption of rubrene monomer. This spontaneous self-assembly of the individual chiral molecules is enantioselective, and results in these two homochiral domains. Figs. 2e and 2f show schematic diagrams for the structural models of the homochiral domain, where all the molecular lattice points reside on the substrate lattice lines along the Si axis. Chiral self-assembly is usually the result of a competition between molecule–substrate interactions and non-covalent intermolecular attractions arising from van der Waals forces, hydrogen bonds, and electrostatic interactions. Combined with the structural model, we consider that the homochiral domain of rubrene can be ascribed to the result of an interplay of van der Waals forces and $\text{CH}\cdots\pi$ interactions arising from the H atoms within the phenyl ring of one molecule and the tetracene backbone of the other molecule (Fig. 2f), which can dominate the weak molecule–substrate interactions on the Bi(111) substrate.

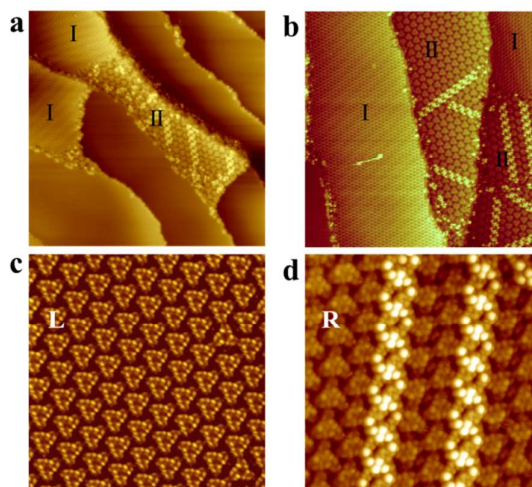


Fig. 3 Homochiral arrangement of individual hexamers formed at the narrow terrace of the Bi(111) surface, coexisting with homochiral domains. (a) Sample area containing two homochiral domains and one triangular hexamer domain, 120 nm × 120 nm, +3.5 V. (b) Another sample area containing two homochiral domain and two triangular hexamer domains, 100 nm × 100 nm, +3.4 V. (c) High-resolution image of L-type triangular hexamer domains, 24.6 nm × 24.6 nm, +3.0 V. (d) High-resolution image of R-type triangular hexamer domains, 29 nm × 29 nm, +2.5 V.

When the homochiral domains of rubrene were annealed to 350 K, a large area of homochiral supramolecular domains with threefold symmetry were discovered at the narrow terrace of the Bi(111) surface, coexisting with the homochiral domains. Figs. 3a and 3b are two different sample areas, containing homochiral domain (type I) and supramolecular structure (type II). From the high resolution STM images of type II domains, the supramolecular structure presented in Fig. 3c consists of triangular chiral clusters with a anticlockwise arrangement (L), whereas the structure in Fig. 3d shows triangular chiral clusters with an clockwise (R) arrangement. As a result, the supramolecular self-assembly are mirror images of each other and can be classified as L- or R-type domains. The lattice of the supramolecular self-assembly was $c_1 = 33.9\text{\AA}$, $c_2 = 33.4\text{\AA}$, $\theta = 60^\circ \pm 0.5^\circ$, and the packing density was 0.63 nm^{-2} , which is larger than that of the homochiral domain. The angle of the high symmetry direction between the supramolecular self-assembly and the substrate was $6^\circ \pm 0.5^\circ$. We speculate that there might be a slight energy difference between the homochiral domain and the supramolecular self-assembly. At elevated temperature, the slight energy difference has been smeared out by thermal fluctuation, leading to the two structures that occurred simultaneously. Rubrene molecules in homochiral domain gain enough energy to seek the lowest energy of the whole system on their own, reconstructing into supramolecular self-assembly at the narrow terrace of Bi(111). By statistical analysis of the domain chirality, almost equal areas of R- and L-type domains were observed on the substrate surface, which suggests an overall achiral surface at the global level. This triangular domain structure is very different from chiral pentagons adsorbed on Au(111)[27] or chiral trimer structures formed on Cu(111)[29].

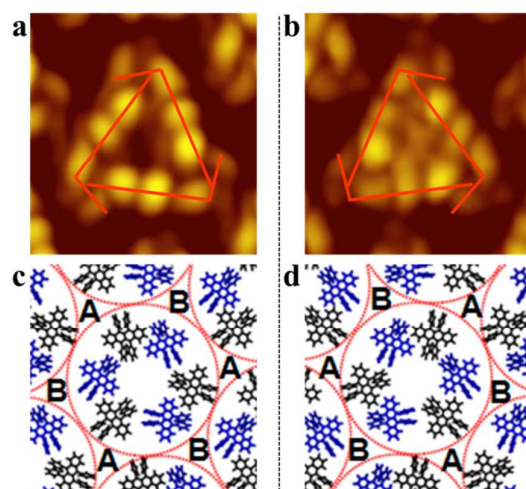


Fig. 4 High-resolution STM images of triangular hexamer structure. (a) A small area of L-type triangular hexamer domain structure, $7.7 \text{ nm} \times 7.7 \text{ nm}$, +2.0 V and (c) the proposed model. (b) A small area of R-type triangular hexamer domain structure, $7.7 \text{ nm} \times 7.7 \text{ nm}$, +2.0 V and (d) the proposed model.

Fig. 4a shows the high-resolution STM image of an L-type triangular unit that we attributed to six heterochiral rubrene molecules. Each side of the triangular structure exhibits four bright protrusions. Within each side, an L-enantiomer rubrene molecule appears as two bright protrusions, whereas an R-enantiomer exhibits two different bright protrusions. Both of the rubrene enantiomers alternate with each other. Consequently, each triangular structure is composed of six rubrene enantiomers as shown in Fig. 4c. It can be conceived that, if the neighboring molecules exchange positions with each other, the L-hexamer will change into its enantiomer, i.e., the R-hexamer, as shown in Fig. 4b. Thus, the rubrene hexamers reveal two levels of organization chirality: one is the six heterochiral rubrene molecules arranged alternatively in rubrene hexamer; and the other is the homochiral arrangement of individual hexamers.

Moreover, the chiral hexamer domains appeared at the narrow terrace of the Bi(111) substrate where strong intermolecular interactions coming from the intense intermolecular squeeze exist. When the homochiral domain was annealed, rubrene molecules began to flow and migrate to the terrace where this molecular flow may become blocked. Therefore, rubrene molecules begin to grind against each other and

undergo a molecular chirality reversal, which are finally reconstructed into chiral hexamer domain structures.

In addition, several bright bands over the triangular domain structures were observed, and we considered these as a second layer of hexamer domains as shown in Fig. 5. The insert of Fig. 5b is the structural model of the second layer. It can be observed that all of the bright bands are aligned along the high symmetry direction of the triangular hexamer structure. The triangular units on each side of the bright bands are rotated by 60° with each other, but keeps the same chirality. As the intermolecular extrusion becomes stronger, rubrene molecules in the first layer are elbowed aside onto the top layer, leading to the formation of bright bands. The formation of bright bands confirms that the intermolecular interplay is strong enough to dominate the substrate–molecule interaction.

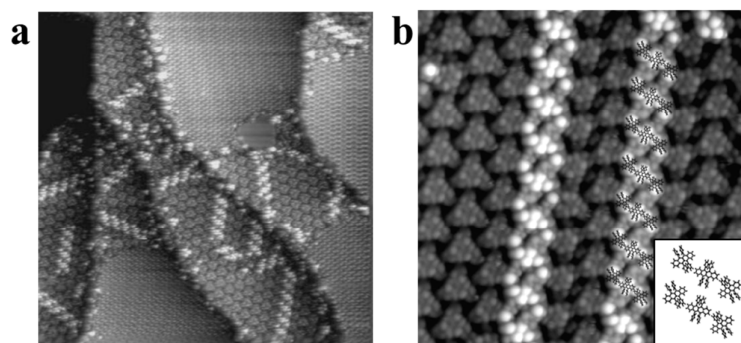


Fig. 5 STM images of hexamer structures with bright bands on the top layer. (a) One sample area containing two self-assembled monolayers and one triangular hexamer structure, $100 \text{ nm} \times 100 \text{ nm}$, $+3.5 \text{ V}$. (b) High-resolution image of R-type domain structure, $28.7 \text{ nm} \times 28.7 \text{ nm}$, $+3.0 \text{ V}$. The insert of (b) is the structural model of the bright bands.

Conclusion

In summary, we identified the absolute configuration of single rubrene enantiomers from high-resolution STM image. Isolated rubrene molecules exhibited an axial chiral adsorption due to the twisted tetracene backbone on the semi-metallic Bi(111) surface. As the coverage increased, two types of homochiral domains composed of rubrene

monomers or hexamers were observed. For rubrene monomers, chiral separation was spontaneous with each chiral monomer appearing in their respective domain. For rubrene hexamers, two levels of organization chirality of six heterochiral rubrene molecules arranged alternatively in rubrene hexamer and the homochiral arrangement of individual hexamers were recorded. By annealing the homochiral domain to 350 K, a large area of supramolecular self-assembled L- and R-type triangular heterochiral hexamers were achieved at the narrow terrace of Bi(111). The formation of hexamer domains can be rationalized by the enhanced intermolecular interactions at the narrow terrace, which dominate the molecule–substrate interactions on the Bi(111) substrate. Moreover, a molecular chiral inversion from L-(R-)type to R-(L-)type occurs during the formation of the hexamer domain structure because of the strong intermolecular interactions governed by the intensive intermolecular extrusion at the narrow terrace. Our findings are significant for supramolecular chirality construction driven by enhanced intermolecular interactions and promote the application of interfacial chiral molecular electronic and optoelectronic devices.

Acknowledgements

This work was supported by the National Natural Science Foundation of China (Grant Nos. 21173170, 10974156, 91121013) and the Fundamental Research Funds for the Central Universities (XDJK2015C151).

References

- 1 S. M. Barlow, R. Raval, *Surf. Sci. Rep.*, 2003, 50, 201–341.
- 2 K. H. Ernst, *Top. Curr. Chem.*, 2006, 265, 209–252.
- 3 R. Raval, *Chem. Soc. Rev.*, 2009, 38(3), 707–721.
- 4 J. A. W. Elemans, I. De Cat, H. Xu and S. De Feyter, *Chem. Soc. Rev.*, 2009, 38(3), 722–736.
- 5 Q. M. Xu, D. Wang, L. J. Wan, et al., *Angew. Chem. Int. Ed.*, 2002, 41(18), 3408–3411.
- 6 G. P. Lopinski, D. J. Moffatt, D. D. M. Wayner and R. A. Wolkow, *Nature*, 1998, 392(6679), 909–911.
- 7 H. B. Fang, L. C. Giancarlo and G. W. Flynn, *J. Phys. Chem. B*, 1998, 102(38), 7311–7315.
- 8 V. Humblot, M. O. Lorenzo, C. J. Baddeley, S. Haq and R. Raval, *J. Am. Chem. Soc.*, 2004, 126(20), 6460–6469.
- 9 M. Parschau, T. Kampen and K. H. Ernst, *Chem. Phys. Lett.*, 2005, 407(4-6), 433–437.
- 10 M. Bohringer, K. Morgenstern, W. D. Schneider and R. Berndt, *Angew. Chem. Int. Ed.*, 1999, 38(6), 821–823.
- 11 I. Paci, I. Szleifer, M. A. Ratner, *J. Am. Chem. Soc.*, 2007, 129(12), 3545–3555.
- 12 T. Huang, Z. P. Hu, A. D. Zhao, H. Q. Wang, B. Wang, J. L. Yang and J. G. Hou, *J. Am. Chem. Soc.*, 2007, 129(13), 3857–3862.
- 13 T. E. Jones, C. J. Baddeley, *Surf. Sci.*, 2002, 519(3), 237–249.
- 14 S. Katano, Y. Kim, H. Matsubara, T. Kitagawa and M. Kawai, *J. Am. Chem. Soc.*, 2007, 129(9), 2511–2515.
- 15 D. G. Yablon, L. C. Giancarlo and G. W. Flynn, *J. Phys. Chem. B*, 2000, 104(32), 7627–7635.
- 16 K. Sun, T. N. Shao, J. L. Xie, M. Lan, Y. H. Yuan, Z. H. Xiong, J. Z. Wang, Y. Liu and Q. K. Xue, *Small*, 2012, 8(13), 2078–2082.
- 17 V. C. Sundar, J. Zaumseil, V. Podzorov, E. Menard, R. L. Willett, T. Someya, M. E. Gershenson and J. A. Rogers, *Science*, 2004, 303, 1644–1646.
- 18 V. Podzorov, E. Menard, A. Borissov, V. Kiryukhin, J. A. Rogers and M. E. Gershenson, *Phys. Rev. Lett.*, 2004, 93, 086602.
- 19 J. Takeya, M. Yamagishi, Y. Tominari, R. Hirahara, Y. Nakazawa, T. Nishikawa, T. Kawase, T. Shimoda and S. Ogawa, *Appl. Phys. Lett.*, 2007, 90, 102120.

- 20 A. L. Briseno, S. C. B. Mannsfeld, M. M. Ling, S. H. Liu, R. J. Tseng, C. Reese, M. E. Roberts, Y. Yang, F. Wudl and Z. N. Bao, *Nature*, 2006, 444, 913-917.
- 21 T. Takahashi, T. Takenobu, J. Takeya and Y. Iwasa, *Appl. Phys. Lett.*, 2006, 88, 033505.
- 22 J. A. Miwa, F. Cicoira, S. Bedwani, J. Lipton-Duffin, D. F. Perepichka, A. Rochefort and F. Rosei, *J. Phys. Chem. C*, 2008, 112, 10214–10221.
- 23 M. C. Blum, E. Cavar, M. Pivetta, F. Patthey and W. D. Schneider, *Angew. Chem. Int. Ed.*, 2005, 44, 5334–5337.
- 24 M. C. Blum, E. Cavar, M. Pivetta, F. Patthey and W. D. Schneider, *Angew. Chem. Int. Ed.*, 2005, 117, 5468–5471.
- 25 M. Pivetta, M. C. Blum, F. Patthey and W. D. Schneider, *J. Phys. Chem. B*, 2009, 113, 4578–4581.
- 26 M. Pivetta, M. C. Blum, F. Patthey and W. D. Schneider, *Angew. Chem. Int. Ed.*, 2008, 47, 1076–1079.
- 27 L. Wang, H. H. Kong, X. Song, X. Q. Liu and H. M. Wang, *Phys. Chem. Chem. Phys.*, 2010, 12, 14682–14685.
- 28 F. Cicoira, J. A. Miwa, D. F. Perepichka and F. Rosei, *J. Phys. Chem. A*, 2007, 111, 12674–12678.
- 29 J. A. Miwa, F. Cicoira, J. Lipton-Duffin, D. F. Perepichka, C. Santato and F. Rosei, *Nanotechnology*, 2008, 19, 424021.
- 30 J. T. Sadowski, T. Nagao, S. Yaginuma, Y. Fujikawa, A. Al-Mahboob, K. Nakajima, T. Sakurai, G. E. Thayer and R.M. Tromp, *Appl. Phys. Lett.*, 2005, 86, 073109.
- 31 G. E. Thayer, J. T. Sadowski, F. Meyer zu Heringdorf, T. Sakurai and R. M. Tromp, *Phys. Rev. Lett.*, 2005, 95, 256106.
- 32 H. Kakuta, T. Hirahara, I. Matsuda, T. Nagao, S. Hasegawa, N. Ueno and K. Sakamoto, *Phys. Rev. Lett.*, 2007, 98, 247601.